https://doi.org/10.5194/egusphere-2025-5945
Preprint. Discussion started: 15 December 2025

Timing of the anthropogenic carbon invasion in the Southern California Current

Yéssica Vanessa Contreras-Pacheco[1,3], Jose Luis Abella Gutiérrez[1,2], Gerardo Vallejo Espinosa[1,3] and Juan Carlos Herguera García[1]*

[1]Division of Oceanography, Center for Scientific Research and Higher Education of Ensenada (CICESE), Ensenada, Mexico

[2] Jackson School of Geosciences, The University of Texas at Austin, Austin, TX, USA

[3]Materials, Water and Energy Research Laboratory, Department of Engineering, University of Guadalajara (UdeG), Tepatitlán de Morelos, Mexico

Corresponding author: *Juan Carlos Herguera (herguera@cicese.mx)

Abstract

The role of Eastern Boundary Upwelling Systems (EBUS), such as the southern California Current System, is a well-known high productivity region driven by alongshore winds, although their role as atmospheric carbon sources and sinks is poorly understood in the global carbon cycle. In the southern CCS, off Baja California, wind-driven vertical mixing upwells nutrient and carbon-rich waters from late winter to early summer, while weaker winds during the rest of the year allow the intrusion of nutrients and carbon-depleted subtropical surface waters. Here, we interpret the isotopic composition of organic carbon and calcitic records spanning 150 years from high-resolution sediment cores collected off Baja California in the context of seasonal variability observed between 1990 and 2011. The results show a clear trend toward lighter carbon isotopic compositions of the organic and inorganic carbon for the past seven decades. These trends are similar to the atmospheric records associated with the Suess effect, suggesting an atmospheric carbon invasion into the surface waters of the California Current. Nevertheless, the slope of the atmospheric carbon isotopic records is steeper than our marine record, most likely related to the upward mixing of subsurface waters with a relatively heavier carbon isotopic signature and advection processes inherent to the strong seasonality of the CCS southern boundary. These results will allow a better characterization of the relative role of the EBUS regions in the global carbon cycle.

https://doi.org/10.5194/egusphere-2025-5945
Preprint. Discussion started: 15 December 2025

1 Introduction

The CO_2 exchange between the ocean and the atmosphere is driven by a combination of physical and biogeochemical processes, making an accurate sea–air CO_2 flux assessment challenging. A better understanding of these processes is necessary to improve our knowledge of the biogeochemical cycles, notably the carbon cycle, which has implications for climate change and ocean acidification (Wanninkhof et al., 2013). Over the past century, the ocean's carbon uptake from the atmosphere has been estimated to be equivalent to 25 to 35 % of the total CO_2 emissions from fossil fuels, cement production, and land use changes, among others (Sabine et al., 2004). This oceanic carbon uptake has slowed down the increase of atmospheric CO_2, reducing the magnitude of the anthropogenically driven climate warming (Fung et al., 2005), and lowered the pH in surface waters with important implications for ocean acidification and marine ecosystems (Feely et al., 2004). Studies of Eastern Boundary Currents (EBUS) have shown that these systems can act as either carbon sources or sinks, depending on the season and latitude (Brady et al., 2019; Chikamoto and DiNezio, 2021; Feely et al., 2008; Lachkar et al., 2024; Lefèvre et al., 2023), making their representation in global carbon models particularly challenging.

The CO_2 released from fossil fuel combustion has a carbon isotopic composition ($\delta^{13}C$) value of -26 to -28 ‰, leading to a decline in the natural atmospheric $\delta^{13}C$ values from approximately -7 ‰ to -8.7 ‰ (Baldwin et al., 2005). This phenomenon, known as the Suess effect (Keeling et al., 1979) is transferred to the ocean through air-sea exchange, and surface and subsurface water masses are the most affected by this perturbation, altering the global oceanic $\delta^{13}C$ distribution (Eide et al., 2017). Therefore, the $\delta^{13}C$ of dissolved inorganic carbon ($\delta^{13}C_{DIC}$) in surface waters is a useful tracer of oceanic uptake of anthropogenic CO_2 (hereafter referred to as C_{ant} uptake) (Sarmiento and Gruber, 2002), and has been previously used to evaluate the uptake and distribution of anthropogenic CO_2 in EBUS (Aguilera et al., 2020; Racapé et al., 2013).

In the surface ocean, biological processes preferentially take up the lighter isotope (^{12}C), shifting its $\delta^{13}C_{DIC}$ towards relatively heavier values, and thermodynamic processes tend to make the $\delta^{13}C_{DIC}$ values in cold waters heavier than those in warm waters via air-sea exchange (Gruber et al., 1999). On the other hand, the uptake of atmospheric carbon by the surface ocean is progressively shifting its $\delta^{13}C_{DIC}$ towards lighter values. Gruber et al. (1999) reported a 15-year-long decrease in $\delta^{13}C$ of -0.25 % per year at the time series station near Bermuda. Depth-integrated analysis from the Atlantic, Indian, and Pacific oceans also shows a decrease in the surface ocean $\delta^{13}C_{DIC}$ for the past few decades (Quay et al., 2003; Quay et al., 2007; Quay et al., 2017).

https://doi.org/10.5194/egusphere-2025-5945
Preprint. Discussion started: 15 December 2025

A high absolute variability in the $\delta^{13}C_{DIC}$ has been observed in the Pacific Ocean basin, linked to the spatiotemporal heterogeneity in CO_2 concentrations, phytoplankton growth rates, and biological production, all influenced by ocean mixing processes (Tagliabue and Bopp, 2008).

Studies in EBUS—such as the California, Humboldt, and Benguela Currents—have shown that $\delta^{13}C_{DIC}$ exhibits marked seasonal and regional variability. During active upwelling periods (spring–summer), the upward transport of CO_2-rich subsurface waters leads to enhanced remineralization and lower $\delta^{13}C_{DIC}$ values at the surface. Conversely, during periods of weaker upwelling, biological fixation of carbon tends to dominate, resulting in relatively higher $\delta^{13}C_{DIC}$ signatures (DeVries, 2014; Ge et al., 2022; Olsen et al., 2020). For instance, in the Humboldt Current System, intensified upwelling events have been associated with lower SST and repeated episodes of $\delta^{13}C_{DIC}$ depletion, consistent with increased contributions of remineralized carbon and reduced biological uptake during these events (Ge et al., 2022).

However, these studies are based on relatively short-term observations that began after significant fossil fuel–derived carbon had already entered the system, complicating efforts to assess the timing and magnitude of oceanic uptake. To better understand the ocean's response to increasing fossil fuel emissions since the late 19th century, it is necessary to rely on paleoceanographic proxies, as instrumental records are too recent to capture long-term trends (Berger et al., 1982).

Planktic foraminifera incorporate DIC from seawater into their calcite shells in near equilibrium with the ambient $\delta^{13}C_{DIC}$ of their preferred surface ocean habitats, typically within the upper tens of meters. This process leaves a stable isotopic signature in their shells that is preserved in sediments and widely used to reconstruct past ocean circulation, carbon reservoir exchange, surface productivity, and nutrient dynamics (Broecker and Peng, 1987; Fairbanks and Wiebe, 1980; Gruber et al., 1999).

The different preferred depth habitats of planktic foraminifera have allowed for the reconstruction of the vertical water column stratification of the ocean by using geochemical proxies for temperature ($\delta^{18}O$, Mg/Ca) and for carbon proxies ($\delta^{13}C$) between near-surface and deeper-dwelling species (Berger, 1971; Emiliani, 1954; Fairbanks and Wiebe, 1980; Ravelo and Fairbanks, 1992; Sautter and Thunell, 1991; Wefer and Berger, 1991). In addition, the organic carbon $\delta^{13}C_{OC}$ also serves as a valuable proxy, as it reflects the photosynthetic conditions under which carbon was fixed, offering insights into past surface CO_2 concentrations (Tagliabue and Bopp, 2008).

The isotopic composition of the organic carbon preserved, mostly derived from phytoplankton, is linked to their physiological function (Young et al., 2013) through the fractionation of preferentially lighter ^{12}C due

https://doi.org/10.5194/egusphere-2025-5945
Preprint. Discussion started: 15 December 2025

to the kinetics of enzymatic processes. $\delta^{13}C_{DIC}$ and $\delta^{13}C_{OC}$ provide complementary information on carbon cycle processes and ocean-atmosphere interactions across multiple timescales. This study uses the ratio of stable isotopes for two phases of carbon, calcite in two species of planktic foraminifera living at different depths, and organic carbon preserved in marine laminated sediments from San Lazaro Basin (SLB), off Baja California, to evaluate the carbon balance between the atmosphere and surface waters in the southern domain of the CCS since the preindustrial era.

2 Materials and methods

2.1 Site description

SLB, sometimes referred to as the Soledad Basin (Van Geen et al., 1995) is located off the western edge of the continental shelf off the Baja California Peninsula (25°10' N, 112°45' W) (Fig. 1). SLB is situated below the dynamic boundary between the cooler and slightly fresher CCS waters advected from the north and the relatively warmer and saltier tropical and subtropical waters from the south (Abella-Gutiérrez and Herguera, 2016). The warmer and saltier tropical and subtropical waters are associated with the poleward advection of the California surface Countercurrent close to the coast (also known as Davison Current), and subsurface nutrients and carbon-enriched and oxygen-depleted waters, with an origin in the equatorial region, known as the California Undercurrent (CUC) (Hickey, 1979).

The CCS shows a strong seasonality, characterized by an intensification of the equatorward alongshore winds during spring to early summer that intensify the advection of the northern cooler and fresher waters of the CC and the upwelling of nutrient and carbon-enriched waters from the subsurface that fuels biological productivity (Lynn and Simpson, 1987; Sverdrup and Allen, 1939) and carbon export (Abella-Gutiérrez et al., 2020; Abella-Gutiérrez and Herguera, 2016). From late summer to early winter, the relaxation of the winds retreats the CC, which allows the invasion of warm stratified Tropical and Subtropical waters in the region, which reduces the biological productivity and carbon export (Durazo, 2015).

This seasonality is enhanced or weakened at different timescales, from interannual to multidecadal, as happens during La Niña-like conditions that extend the spring upwelling and El Niño-like conditions that

https://doi.org/10.5194/egusphere-2025-5945
Preprint. Discussion started: 15 December 2025

enhance stratification throughout the year (Abella-Gutiérrez et al., 2020; Durazo, 2015; O'Mara et al., 2019).

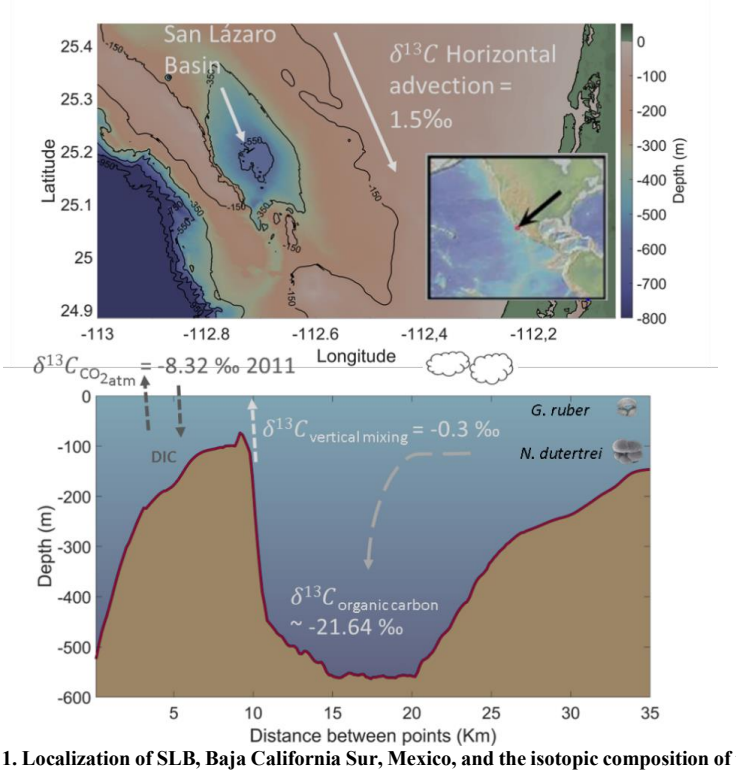

Figure 1. Localization of SLB, Baja California Sur, Mexico, and the isotopic composition of the main processes that imprint the δ13C to the DIC in the mixed layer. The above image was generated from GeoMapApp using the Global Multi-Resolution Topography (Ryan, et al., 2009) with modifications.

SLB has a maximum depth of ~540 m and is enclosed in its western margin by an uplifted branch of the Tosco-Abreojos fault system with depths around 100 m that is broken by a narrow sill of 350 m depth (

Figure 1. Localization of SLB, Baja California Sur, Mexico, and the isotopic composition of the main processes that imprint the δ13C to the DIC in the mixed layer. The above image was generated from GeoMapApp using the Global Multi-Resolution Topography (Ryan, et al., 2009) with modifications.). The reduced ventilation over the sill, the oxygen-depleted waters of the CUC entering the basin through these depths, and the high productivity help to maintain the suboxic conditions on the seafloor that prevent bioturbation and enhance the preservation of the laminated sediments accumulating on its bottom (Juillet-Leclerc and Schrader, 1987; Phleger and Soutar, 1973; Thunell, 1998; Van Geen et al., 1995).

https://doi.org/10.5194/egusphere-2025-5945
Preprint. Discussion started: 15 December 2025

2.2 Sample collection

Two box cores (SALA11-E19MC-1 and BAP96-6C) were collected (Table 1) from the deepest part of the basin, with a Soutar-type box core that recovered a well-preserved sediment-water interface. We made further use of the top section of the Kasten core (PCM00-78K), which was previously employed in earlier studies, to describe the CCS, sea surface temperature (SST), and paleoproductivity variability (Abella-Gutiérrez et al., 2020; Abella-Gutiérrez and Herguera, 2016; O'Mara et al., 2019) to extend the record back to the preindustrial era.

After recovery, the cores were refrigerated until sampling in the lab, where they were cut into 2 cm slabs along the depth axis. Several slabs were archived and X-radiographed, and the rest were continuously sampled perpendicular to the depth axis at 2-3 mm resolution, roughly translating into 1–4 year time slices.

Two species of planktic foraminifera preserved in the sediments were selected for analysis: *Neogloboquadrina dutertrei* and *Globigerinoides ruber*. *G. ruber* is a spinose species known to be colonized with symbionts under relatively higher light conditions, close to the surface of the water column, and has been reported to occupy a near-surface niche (Gastrich and Bartha, 1988), whereas *N. dutertrei* is a non-spinose species mostly found within the upper seasonal thermocline, usually closely associated with the depth of the chlorophyll maximum in the CC (Field, 2004; Sautter and Thunell, 1991; Spindler et al., 1984).

Table 1. Localization and year of the collected cores in SLB

Core	Latitude	Longitude	Depth	Year	Type
SALA11-E19MC-1	25.1961 N	112.7986 W	-540 m	2011	Soutar box core
PCM00-78K	25.1883 N	112.6783 W	-540 m	2000	Kasten
BAP96-6C	25.2163 N	112.7333 W	-528 m	1996	Soutar box core

2.3 Stable isotopic determinations on carbonates and organic carbon

To determine the $\delta^{13}C_{calc}$, we used selected planktic foraminifera from cores SALA11-E19MC-1 and BAP96-6C. Freeze-dried samples were disaggregated in a solution of sodium hexametaphosphate. The sediment was washed through a 64 µm sieve mesh and then transferred and treated with a 3 % hydrogen peroxide (H_2O_2) in an ultrasonic bath for 3 minutes to help disaggregate the sediment samples to pick planktic foraminifera.

https://doi.org/10.5194/egusphere-2025-5945
Preprint. Discussion started: 15 December 2025

Once dried, we handpicked specimens of planktic foraminifera *N. dutertrei* and *G. ruber* from the 250-350 µm fraction; the number of specimens per species is approximately 14 shells needed to weigh a minimum total of 140 µg of carbonate per sample. These were placed in Exetainer tubes and dried at 110 °C for 24 h. Once at room temperature, the air was evacuated with ultra-pure helium (99.99 %).

After closing the Exetainer, we injected ~0.05 ml of 99 % orthophosphoric acid to dissolve the foraminifera tests, and the resulting carbon dioxide was carried with He to a gas chromatograph (GasBench II®) coupled to a DeltaPlus Advantage® mass. Each run of 45 samples was accompanied by two international reference standards, NBS19 and LSVEC, and laboratory internal references. The average precision from certified values during the runs was ±0.06‰ for $\delta^{13}C$ for both standards and four internal laboratory standards. Results are reported as δ values with reference to the international standard VPDB.

$$\delta^{13}C(‰) = \left(\frac{R_{sample}}{R_{standard}} - 1\right) \times 1000 \quad (1)$$

Where R is the $^{13}C/^{12}C$ ratio, and the "standard" refers to PDB belemnite.

To determine the $\delta^{13}C_{Corg}$ in the sediment samples, we analyzed 330 samples from the three cores described above. Samples were freeze-dried, and the carbonate component was dissolved with dilute hydrochloric acid (HCl). We added deionized water and centrifuged the samples to discard the supernatant, after which these were dried and encapsulated to determine their $\delta^{13}C_{Corg}$ composition.

Samples were loaded in a carousel and combusted in an oxygen atmosphere in a COSTECH elemental analyzer coupled to a Thermo DeltaV Advantage IR mass spectrometer in the Laboratorio de Isótopos Estables (LIE) at CICESE. Each run of 30 samples was accompanied by international reference standards USGS 40 (L-glutamic acid) and Sucrose ANU, and internal laboratory references, with average precision from certified values of ±0.06‰ for both standards, as well as six internal laboratory standards, reported as δ values with reference to the international standard VPDB.

$$\delta^{13}C_{Corg}(‰, VPDB) = \left(\frac{R_{sample}}{R_{standard}} - 1\right) \times 1000 \quad (2)$$

Where R is the $^{13}C/^{12}C$ ratio, and the "standard" refers to VPDB belemnite.

2.4 Age model

The core BAP96-6C was radiometrically dated by excess ^{210}Pb, and the presence of the isotope ^{137}Cs was reported in (Esparza-Alvarez et al., 2007). Core PCM00-78K was dated using radiocarbon measurements,

https://doi.org/10.5194/egusphere-2025-5945
Preprint. Discussion started: 15 December 2025

as detailed in Abella-Gutiérrez et al., 2020. Core SALA11-E19MC-1 was stratigraphically correlated with the carbonate record of BAP96-6C (as shown in the supplementary material, Figure S1).

2.5 Data analysis

To understand the behavior of this region of the CC and its role in carbon cycling, particularly the C_{ant} uptake relative to the atmosphere over a year, we calculated the CO_2 fugacity (fCO_2) in seawater using the data from the Surface Ocean CO_2 Atlas (Bakker, et al., 2016) between 1990 and 2011. We gathered all the existing data points over 12 months (Figure 2).

To characterize the $\delta^{13}C$ variability in the upper water column, we analyzed $\delta^{13}C$ of *N. dutertrei* ($\delta^{13}C_{Nd}$) and *G. ruber* ($\delta^{13}C_{Gr}$), preserved in cores SALA11-E19MC-1 and BAP96-6C, respectively (Figure 1). The combined use of modern CO_2 observations and $\delta^{13}C$ records from species occupying different depth habitats allows for a complementary approach to assess past and present carbon cycling, providing insights into vertical variability in carbon uptake and redistribution.

We applied two complementary approaches to reconstruct the $\delta^{13}C_{DIC}$ in the water column. First, we averaged the $\delta^{13}C_{Corg}$ values from the 1800-1940 time series and used the data to derive a phytoplankton fractionation factor of –21‰. Second, we used the $\delta^{13}C_{calc}$ from *G. ruber and N. dutertrei,* assuming isotopic equilibrium fractionation at the depths where each species calcifies. We estimated the $\delta^{13}C_{DIC}$ yearly by subtracting the organic carbon fractionation factor from the corresponding $\delta^{13}C_{calc}$. This difference represents the inferred $\delta^{13}C_{DIC}$ throughout the water column.

3 Results

3.1 Seasonal variability

The seasonal variability of CO_2 fugacity in seawater shows that the surface waters act as a carbon source between July and November, while the rest of the year, the surface waters act as a sink, with most of the values below 400 µatm (Figure 2-A). The observed internal variability in surface waters (ρCO_2) is apparently phase locked with the seasonal cycle, as the observed fluctuations of internal variability closely track the peaks and troughs of the seasonal SSTs in this region. This upwelling region shows ρCO_2 maxima, and thus CO_2 outgassing, in August-September and its minimum ρCO_2 (and thus CO_2 uptake) in April-May.

https://doi.org/10.5194/egusphere-2025-5945
Preprint. Discussion started: 15 December 2025

This seasonal cycle has a thermal component, driven by the seasonality of SST, and a non-thermal component driven by the seasonality of other factors such as DIC and alkalinity (Takahashi et al., 2002). These observations suggest that the phase of the seasonal cycle of this upwelling region in the southern CCS is partly controlled by thermal (solubility) effects. However, the large scatter observed during late summer to fall may be modulated by non-thermal factors (Figure 2-A). These non-thermal factors may be driven by the seasonal cycle of DIC modulated by photosynthetic uptake of CO_2 and respiration processes in the summer and fall.

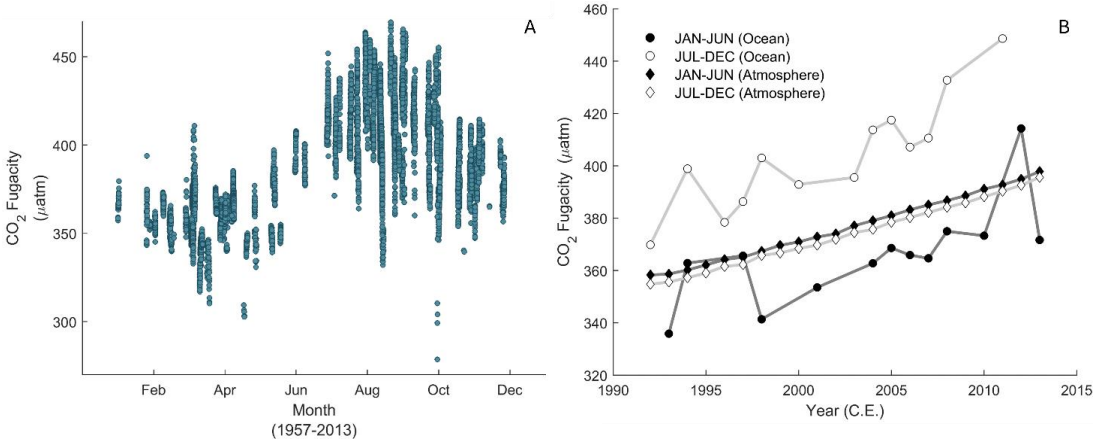

Figure 2. Seasonal and interannual variability of CO_2 in surface waters of the southern California Current, based on SOCAT data (Bakker et al., 2016). (A) Seasonal cycle from 1957 to 2013. (B) Annual average fCO_2 time series (1993–2013): January–June (solid blue), July–December (solid grey), and atmospheric values from Mauna Loa (dotted blue and grey).

The time series averages for the winter to late spring period of 1993-2013 (Figure 2-B) consistently show an offset of ±20 µatm above and below the CO_2 concentrations measured at the Mauna Loa station (Global Monitoring Laboratory - Carbon Cycle Greenhouse Gases, 2024).

Seasonally, the surface waters exhibit a consistent positive offset ranging from +20 to +25 µatm from July to November, relatively higher SSTs, and a negative offset between -10 to -15 µatm from winter to spring, coincident with the lower SSTs. In both cases, there is a clear trend towards higher ρCO_2 values for both ocean seasons throughout the past 20 years of the record, following the upward trend observed for the atmospheric CO_2 for the same period.

3.2 Long-term ocean-atmosphere carbon exchange

The reconstructed isotopic compositions of organic carbon from cores PCM-78K, SALA11-E19MC-1, and BAP96-6C show minor oscillations around mean values of -21 ‰ between 1850 and 1950 and a marked

https://doi.org/10.5194/egusphere-2025-5945
Preprint. Discussion started: 15 December 2025

trend toward more negative values as we approach the present period (Figure 3). Similarly, $\delta^{13}C_{Nd}$ and $\delta^{13}C_{Gr}$ time series exhibit a similar change towards lighter values around the 1950s. However, these trends in our proxy records show a lower slope than the atmospheric trend (Figure 4), suggesting that additional processes influence the isotopic composition in the marine sediments.

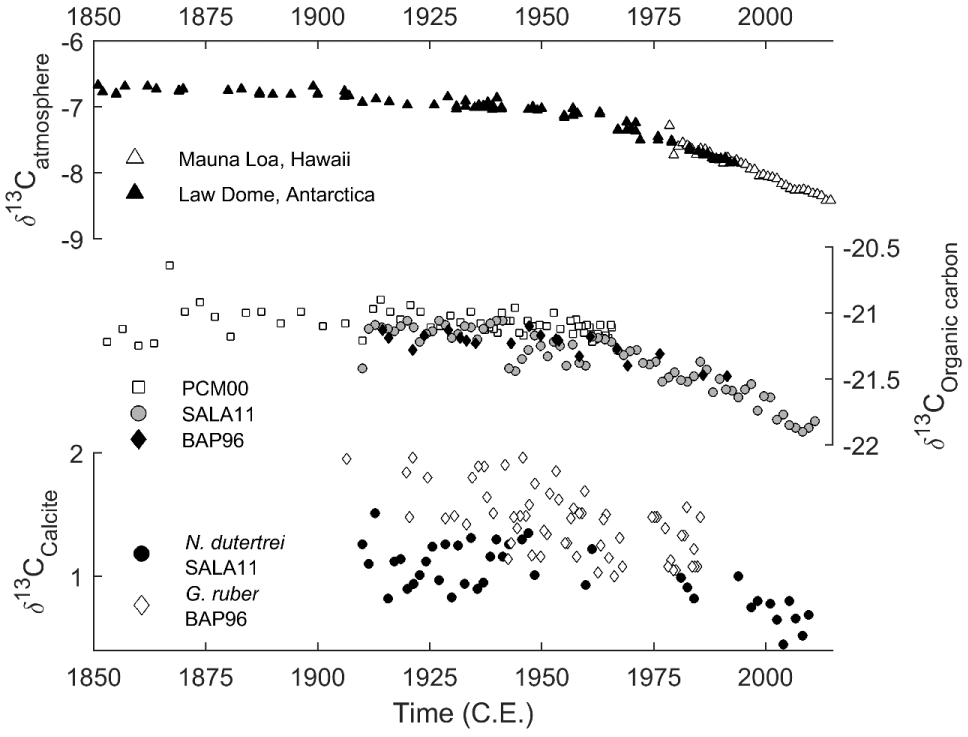

Figure 3. Time series of the carbon isotopic composition are presented in three sections: the upper panel illustrates the atmospheric reservoir from an ice core (Rubino et al., 2019) and instrumental data (Keeling et al., 2001). The middle panel shows the organic carbon phase obtained from sediment cores, and in the lower panel, the calcite phase obtained from planktic foraminifera *N. dutertrei* and *G. ruber* from sediment cores.

https://doi.org/10.5194/egusphere-2025-5945
Preprint. Discussion started: 15 December 2025

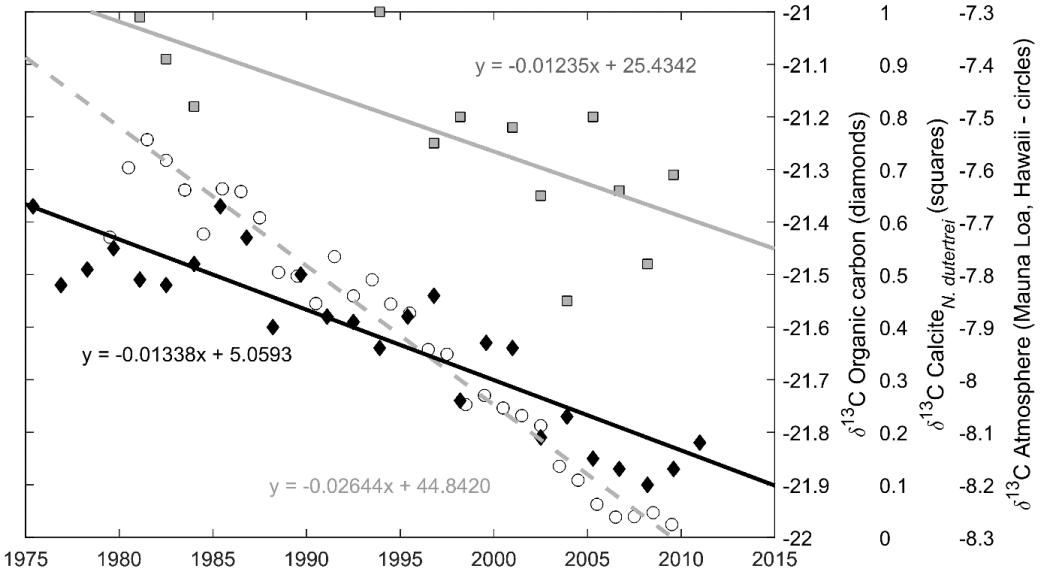

225

Figure 4. Time series slopes of $\delta^{13}C_{atm}$ (hollow circles), $\delta^{13}C_{Nd}$ of *N. dutertrei* (solid black diamonds), and $\delta^{13}C_{Corg}$ (solid gray squares) between 1975 and 2011.

226 To understand the controls on variability in $\delta^{13}C_{Corg}$ and $\delta^{13}C_{Nd}$, we reconstructed the $\delta^{13}C_{DIC}$, from $\delta^{13}C_{Corg}$
227 using a constant fractionation factor (ε=-21‰), corresponding to the mean isotopic offset between organic
228 and dissolved inorganic carbon during 1800 to 1940. The reconstructed $\delta^{13}C_{DIC}$ values were then compared
229 with the inorganic carbon of planktic foraminifera preserved in sediments (Figure 5). Our reconstructed
230 $\delta^{13}C_{DIC}$ shows intermediate values and follows the same trend as planktic foraminifera $\delta^{13}C$, suggesting that
231 it reflects the integrated productivity of the mixed layer and water column. This also indicates that the long-
232 term trend observed in $\delta^{13}C_{Corg}$ is a reliable tracer of upper-ocean $\delta^{13}C_{DIC}$ variability.

https://doi.org/10.5194/egusphere-2025-5945
Preprint. Discussion started: 15 December 2025

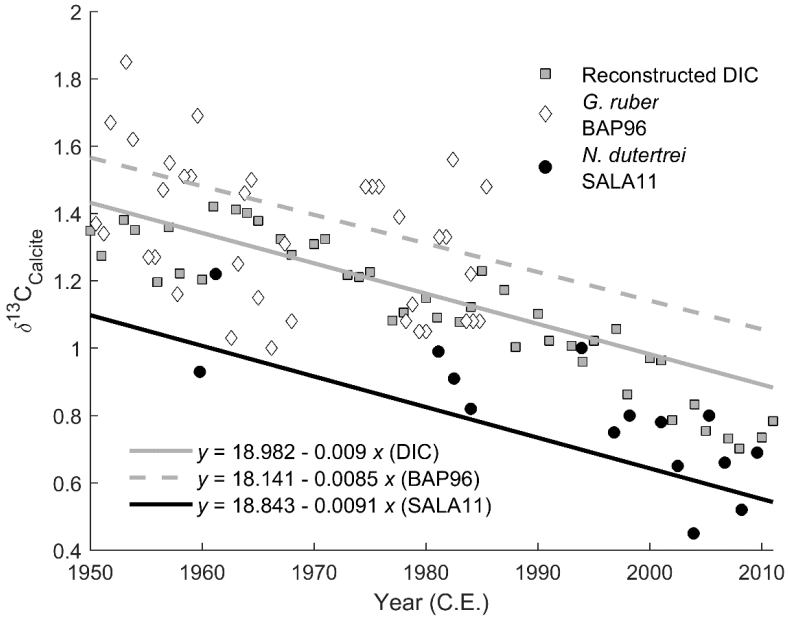

Figure 5. Time series and trends of the carbon isotopic composition of *G. ruber* (open diamonds) and *N. dutertrei* (black circles), as well as the DIC (grey squares), are derived from organic carbon in the sediments.

4 Discussions

The reconstructed $\delta^{13}C$ of both organic carbon and calcite follows similar decreasing trends to the observed (Keeling et al., 2001) and reconstructed (Rubino et al., 2019) values of the atmosphere (Figure 3), associated with the Suess effect, driven by the combustion of fossil fuels (Keeling et al., 1979, 2001; Tans, 2022). However, the shallower slope found in our proxies ($\delta^{13}C_{Corg}$ and $\delta^{13}C_{Nd}$) suggests other processes are involved, most likely related to the seasonal source and sink roles of EBUS regions on the carbon cycle.

Influenced by seasonal upwelling, our study area represents a complex setting for interpreting $\delta^{13}C$ variability. Upwelling introduces relatively heavier $\delta^{13}C$ DIC-rich waters to the surface ocean, potentially buffering the lighter isotopic composition of atmospheric CO_2 ($\delta^{13}C_{atm}$) of the Suess effect (Tagliabue and Bopp, 2008; Quay et al., 2017). In these regions, $\delta^{13}C$ values in surface waters are controlled on the one hand by air–sea CO_2 exchange and by respiration processes of organic matter and the DIC content of upwelled waters. As observed in our proxy records, this mixture of sources most likely leads to $\delta^{13}C$ signals that diverge from atmospheric trends, particularly in eastern boundary current systems like the California Current.

https://doi.org/10.5194/egusphere-2025-5945
Preprint. Discussion started: 15 December 2025

The $\delta^{13}C_{calc}$ trends of planktic foraminifera calcite show a slope of -0.12‰ per decade since 1970, while the $\delta^{13}C_{Corg}$ shows a slope of -0.15‰ per decade. These values lie at the low range of variability previously reported of -0.20±0.06 decade^{-1} for the North Pacific, which is already lower than the 0.27‰ decade^{-1} observed for the atmospheric CO_2 (Quay et al., 2017). According to Gruber et al., (1999) the highest Suess effect, -0.25 ‰ decade^{-1}, is found in the subtropical gyres such as Bermuda and Hawaii, whereas the lowest, -0.15 ‰ decade^{-1}, is found in the equatorial Pacific upwelling region. Our study region shows a decreasing decadal trend similar to the equatorial region, characteristic of its strong upwelling. Although temperature-dependent fractionation and total CO_2 fluxes are relevant, most observed trends towards lighter values in the surface ocean $\delta^{13}C_{DIC}$ can be attributed to the input of $\delta^{13}C_{atm}$. Therefore, understanding the spatial distribution of the $\delta^{13}C$ Suess effect requires considering ocean mixing and circulation patterns (Tagliabue and Bopp, 2008).

Surface ocean $\delta^{13}C$ is mainly controlled by input of atmospheric CO_2 either through air–sea exchange or lateral advection of anthropogenic CO_2, the export of organic matter, respiration processes in the surface layer, the lateral advection of DIC, and mixing from subsurface waters. This intrusion of isotopically light atmospheric CO_2 into the ocean tends to erase natural $\delta^{13}C$ gradients (Eide et al., 2017), and consequently the variability of the $\delta^{13}C_{CDIC}$ downstream of upwelling zones introduced by primary productivity, upwelling of older water, and $\delta^{13}C_{atm}$ (Tagliabue and Bopp, 2008).

Our results clearly show this mixture of influences, as our proxies are partially tracking the atmospheric signal. Tracking the propagation of the Suess effect across Earth system components offers insights into the magnitude of anthropogenic CO_2 sinks (Eide et al., 2017). Gruber et al. (1999) estimated that the global oceanic $\delta^{13}C$ Suess effect closely matches the atmospheric trend. In contrast, Tagliabue and Bopp (2008) reported $\delta^{13}C_{DIC}$ decline rates of −0.07‰ per decade between 1860 and 2000, increasing to −0.18‰ per decade between 1970 and 2000. Observations for 1970–1990 show ocean $\delta^{13}C_{DIC}$ changes of −0.15 to −0.171‰ per decade, representing roughly 65% of the $\delta^{13}C_{atm}$ decrease.

Although atmospheric inputs primarily drive the propagation of the $\delta^{13}C$ Suess effect into the surface ocean, its oceanic expression is modulated by regional circulation, upwelling dynamics, and biological productivity. For instance, the upwelling of older, relatively heavier $\delta^{13}C$ deep waters, as observed in our study area, can offset the surface signal. If fossil-fuel-driven atmospheric changes were the only process involved, $\delta^{13}C_{Corg}$ and $\delta^{13}C_{Nd}$ would closely follow atmospheric trends. While upwelling delivers remineralized DIC with a heavier $\delta^{13}C$ than the atmospheric, depending on the age and origin of the water mass. This dual effect may partially buffer the surface $\delta^{13}C$ Suess signal in regions such as the California

https://doi.org/10.5194/egusphere-2025-5945
Preprint. Discussion started: 15 December 2025

Current (Tagliabue and Bopp, 2008; Quay et al., 2017). The mismatch in slope between atmospheric and marine $\delta^{13}C$ records reflects the role of other oceanic processes, such as lateral and subsurface mixing with the upper ocean mixed layer, as well as the integration of multiple carbon pools, including organic matter, upper ocean DIC, and pathways driven by biological productivity in the surface light waters. Our data reinforce that sedimentary $\delta^{13}C$ reflects a regional imprint of global carbon cycle perturbations, modulated by local oceanographic processes.

Upwelling regions like the southern California Current play a central role in shaping the marine isotopic carbon signal. The persistence of seasonal source/sink behavior in surface waters (Figure 2) likely contributes to the lower slope observed in sediment $\delta^{13}C$ values. Although the Suess effect dominates the long-term trend, its regional expression depends on the balance between atmospheric CO_2 uptake and the delivery of older DIC from depth. As Le Quéré et al. (2018) emphasize, regional systems with dynamic vertical and horizontal transport processes are key components of the global carbon cycle and crucial to understanding the propagation of anthropogenic CO_2 through the ocean-atmosphere system.

4 Conclusions

The $\delta^{13}C$ trends of planktic foraminifera calcite and organic carbon in our study, with slopes of −0.12‰ and −0.15‰ per decade, respectively, lie at the lower end of the variability reported for the North Pacific, although similar to the decadal rates reported for the equatorial Pacific, and remain consistently below the $\delta^{13}C_{atm}$ trend. These findings reflect the global imprint of the ^{13}C Suess effect and the influence of regional oceanographic processes such as mixing subsurface waters driven by upwelling processes.

The $\delta^{13}C$ trend mismatch observed in marine sediments with respect to the atmospheric ones suggests a combined effect of anthropogenic CO_2 atmospheric source, and the upwelling of intermediate waters with relatively enriched $\delta^{13}C$ signatures relative to the atmospheric values, in the California Current. These mechanisms modulate the isotopic imprint of atmospheric CO_2 on the ocean, leading to spatial heterogeneity in the marine $\delta^{13}C$ response.

Temporal patterns further confirm that the oceanic $\delta^{13}C$ response partially buffers the atmospheric trend, highlighting the role of ocean circulation and ventilation timescales. The discrepancy between sediment $\delta^{13}C$ records (Figure 4) and atmospheric ones underscores the need to consider the integration of multiple carbon pools and processes—such as biological export, remineralization, and lateral transport—when interpreting long-term isotopic trends in the ocean sediment records.

https://doi.org/10.5194/egusphere-2025-5945
Preprint. Discussion started: 15 December 2025

Our results emphasize the importance of the anthropogenic source of carbon to alter the oceanic carbon isotopic composition of the ocean, and how this trend has been significantly shifting in the CCS ever since the 1950s, mirroring the atmospheric CO_2 trend captured in the Law Dome ice core record in Antarctica.

Author contributions

YC: First author, laboratory and data analysis, data curation, and conceptualization. JA: Data analysis and writing. GV: Data analysis and writing. JH: Conceptualization, supervision, investigation, methodology, data curation, resources, project administration, funding acquisition, writing-review and editing, manuscript improvement. All authors contributed to the article and approved the submitted version.

Funding

Y.V. Contreras-Pacheco was supported by a CONAHCYT Master's and PhD fellowship.

Acknowledgments

We thank Cynthia Nava, Bertha Acosta, Axel Rosas, Aidé Egremy, Mireya Montero, Nathali Cordero, and Doreny Bobadilla for their help in the collection and the laboratory work. We also thank Gerardo Quintanilla for his feedback during the earlier stages. We thank the crew of the R/V Francisco Ulloa for their support. This study has been conducted using E.U. Copernicus Marine Service Information.

Competing interests

The contact author has declared that none of the authors has any competing interests.

References

Abella-Gutiérrez, J. and Herguera, J. C.: Sensitivity of carbon paleoproductivity in the Southern California Current System on different time scales for the last 2 ka: CARBON PALEOPRODUCTIVITY IN THE SOUTHERN CCS, Paleoceanography, 31, 953–970, https://doi.org/10.1002/2015PA002872, 2016.

Abella-Gutiérrez, J., Herguera, J. C., Mortyn, P. G., Kelly, C. S., and Martínez-Botí, M. A.: Multidecadal Climate Variability in the Southern Region of the California Current System During the Last 1,800 Years, Paleoceanogr. Paleoclimatology, 35, e2019PA003825, https://doi.org/10.1029/2019PA003825, 2020.

Aguilera, V. M., Vargas, C. A., and Dewitte, B.: Intraseasonal Hydrographic Variations and Nearshore Carbonates System Off Northern Chile During the 2015 El Niño Event, J. Geophys. Res. Biogeosciences, 125, e2020JG005704, https://doi.org/10.1029/2020JG005704, 2020.

Bakker, D. C. E., Pfeil, B., Landa, C. S., Metzl, N., O'Brien, K. M., Olsen, A., Smith, K., Cosca, C., Harasawa, S., Jones, S. D., Nakaoka, S., Nojiri, Y., Schuster, U., Steinhoff, T., Sweeney, C., Takahashi, T., Tilbrook, B., Wada, C.,

https://doi.org/10.5194/egusphere-2025-5945
Preprint. Discussion started: 15 December 2025

Wanninkhof, R., Alin, S. R., Balestrini, C. F., Barbero, L., Bates, N. R., Bianchi, A. A., Bonou, F., Boutin, J., Bozec, Y., Burger, E. F., Cai, W.-J., Castle, R. D., Chen, L., Chierici, M., Currie, K., Evans, W., Featherstone, C., Feely, R. A., Fransson, A., Goyet, C., Greenwood, N., Gregor, L., Hankin, S., Hardman-Mountford, N. J., Harlay, J., Hauck, J., Hoppema, M., Humphreys, M. P., Hunt, C. W., Huss, B., Ibánhez, J. S. P., Johannessen, T., Keeling, R., Kitidis, V., Körtzinger, A., Kozyr, A., Krasakopoulou, E., Kuwata, A., Landschützer, P., Lauvset, S. K., Lefèvre, N., Lo Monaco, C., Manke, A., Mathis, J. T., Merlivat, L., Millero, F. J., Monteiro, P. M. S., Munro, D. R., Murata, A., Newberger, T., Omar, A. M., Ono, T., Paterson, K., Pearce, D., Pierrot, D., Robbins, L. L., Saito, S., Salisbury, J., Schlitzer, R., Schneider, B., Schweitzer, R., Sieger, R., Skjelvan, I., Sullivan, K. F., Sutherland, S. C., Sutton, A. J., Tadokoro, K., Telszewski, M., Tuma, M., Van Heuven, S. M. A. C., Vandemark, D., Ward, B., Watson, A. J., and Xu, S.: A multi-decade record of high-quality <i>f</i>CO₂ data in version 3 of the Surface Ocean CO₂ Atlas (SOCAT), Earth Syst. Sci. Data, 8, 383–413, https://doi.org/10.5194/essd-8-383-2016, 2016.

Baldwin, I. T., Caldwell, M. M., Heldmaier, G., Jackson, R. B., Lange, O. L., Mooney, H. A., Schulze, E.-D., Sommer, U., Ehleringer, J. R., Denise Dearing, M., and Cerling, T. E. (Eds.): A History of Atmospheric CO2 and Its Effects on Plants, Animals, and Ecosystems, Springer New York, New York, NY, https://doi.org/10.1007/b138533, 2005.

Berger, W., Bonneau, M., and Parker, F.: Foraminifera on the deep-sea floor - lysocline and dissolution rate, Oceanol. Acta, 5, 249–258, 1982.

Berger, W. H.: Sedimentation of planktonic foraminifera, Mar. Geol., 11, 325–358, https://doi.org/10.1016/0025-3227(71)90035-1, 1971.

Brady, R. X., Lovenduski, N. S., Alexander, M. A., Jacox, M., and Gruber, N.: On the role of climate modes in modulating the air–sea CO_2 fluxes in eastern boundary upwelling systems, Biogeosciences, 16, 329–346, https://doi.org/10.5194/bg-16-329-2019, 2019.

Broecker, W. S. and Peng, T.-H.: The role of $CaCO_3$ compensation in the glacial to interglacial atmospheric CO_2 change, Glob. Biogeochem. Cycles, 1, 15–29, https://doi.org/10.1029/GB001i001p00015, 1987.

Chikamoto, M. O. and DiNezio, P.: Multi-Century Changes in the Ocean Carbon Cycle Controlled by the Tropical Oceans and the Southern Ocean, Glob. Biogeochem. Cycles, 35, e2021GB007090, https://doi.org/10.1029/2021GB007090, 2021.

DeVries, T.: The oceanic anthropogenic CO_2 sink: Storage, air-sea fluxes, and transports over the industrial era, Glob. Biogeochem. Cycles, 28, 631–647, https://doi.org/10.1002/2013GB004739, 2014.

Durazo, R.: Seasonality of the transitional region of the California Current System off Baja California, J. Geophys. Res. Oceans, 120, 1173–1196, https://doi.org/10.1002/2014JC010405, 2015.

Eide, M., Olsen, A., Ninnemann, U. S., and Eldevik, T.: A global estimate of the full oceanic 13C Suess effect since the preindustrial, Glob. Biogeochem. Cycles, 31, 492–514, https://doi.org/10.1002/2016GB005472, 2017.

Emiliani, C.: Depth habitats of some species of pelagic Foraminifera as indicated by oxygen isotope ratios, Am. J. Sci., 252, 149–158, https://doi.org/10.2475/ajs.252.3.149, 1954.

Esparza-Alvarez, M. A., Herguera, J. C., and Lange, C.: Last century patterns of sea surface temperatures and diatom (>38 μm) variability in the Southern California current, Mar. Micropaleontol., 64, 18–35, https://doi.org/10.1016/j.marmicro.2007.01.001, 2007.

Fairbanks, R. G. and Wiebe, P. H.: Foraminifera and Chlorophyll Maximum: Vertical Distribution, Seasonal Succession, and Paleoceanographic Significance, Science, 209, 1524–1526, https://doi.org/10.1126/science.209.4464.1524, 1980.

https://doi.org/10.5194/egusphere-2025-5945
Preprint. Discussion started: 15 December 2025

Feely, R. A., Sabine, C. L., Lee, K., Berelson, W., Kleypas, J., Fabry, V. J., and Millero, F. J.: Impact of Anthropogenic CO_2 on the $CaCO_3$ System in the Oceans, Science, 305, 362–366, https://doi.org/10.1126/science.1097329, 2004.

Feely, R. A., Sabine, C. L., Hernandez-Ayon, J. M., Ianson, D., and Hales, B.: Evidence for Upwelling of Corrosive "Acidified" Water onto the Continental Shelf, Science, 320, 1490–1492, https://doi.org/10.1126/science.1155676, 2008.

Field, D. B.: Variability in vertical distributions of planktonic foraminifera in the California Current: Relationships to vertical ocean structure: VERTICAL VARIABILITY OF FORAMINIFERA, Paleoceanography, 19, n/a-n/a, https://doi.org/10.1029/2003PA000970, 2004.

Fung, I. Y., Doney, S. C., Lindsay, K., and John, J.: Evolution of carbon sinks in a changing climate, Proc. Natl. Acad. Sci., 102, 11201–11206, https://doi.org/10.1073/pnas.0504949102, 2005.

Gastrich, M. D. and Bartha, R.: Primary productivity in the planktonic foraminifer Globigerinoides ruber (d'Orbigny), J. Foraminifer. Res., 18, 137–142, https://doi.org/10.2113/gsjfr.18.2.137, 1988.

Ge, T., Luo, C., Ren, P., Zhang, H., Fan, D., Chen, H., Chen, Z., Zhang, J., and Wang, X.: Stable carbon isotopes of dissolved inorganic carbon in the Western North Pacific Ocean: Proxy for water mixing and dynamics, Front. Mar. Sci., 9, 998437, https://doi.org/10.3389/fmars.2022.998437, 2022.

Gruber, N., Keeling, C. D., Bacastow, R. B., Guenther, P. R., Lueker, T. J., Wahlen, M., Meijer, H. A. J., Mook, W. G., and Stocker, T. F.: Spatiotemporal patterns of carbon-13 in the global surface oceans and the oceanic suess effect, Glob. Biogeochem. Cycles, 13, 307–335, https://doi.org/10.1029/1999GB900019, 1999.

Hickey, B. M.: The California current system—hypotheses and facts, Prog. Oceanogr., 8, 191–279, https://doi.org/10.1016/0079-6611(79)90002-8, 1979.

Juillet-Leclerc, A. and Schrader, H.: Variations of upwelling intensity recorded in varved sediment from the Gulf of California during the past 3,000 years, Nature, 329, 146–149, https://doi.org/10.1038/329146a0, 1987.

Keeling, C. D., Mook, W. G., and Tans, P. P.: Recent trends in the 13C/12C ratio of atmospheric carbon dioxide, Nature, 277, 121–123, https://doi.org/10.1038/277121a0, 1979.

Keeling, C. D., Piper, S. C., Bacastow, R. B., Wahlen, M., Whorf, T. P., Heimann, M., and Meijer, H. A.: Exchanges of Atmospheric CO2 and 13CO2 with the Terrestrial Biosphere and Oceans from 1978 to 2000. I. Global Aspects, 2001.

Lachkar, Z., Cornejo-D'Ottone, M., Singh, A., Arístegui, J., Dewitte, B., Fawcett, S., Garçon, V., Lovecchio, E., Molina, V., and Vinayachandran, P. N. M.: Biogeochemistry of greenhouse gases in coastal upwelling systems: Processes and sensitivity to global change, Elem Sci Anth, 12, 00088, https://doi.org/10.1525/elementa.2023.00088, 2024.

Lefèvre, N., Veleda, D., and Hartman, S. E.: Outgassing of CO2 dominates in the coastal upwelling off the northwest African coast, Deep Sea Res. Part Oceanogr. Res. Pap., 200, 104130, https://doi.org/10.1016/j.dsr.2023.104130, 2023.

Lynn, R. J. and Simpson, J. J.: The California Current system: The seasonal variability of its physical characteristics, J. Geophys. Res., 92, 12947, https://doi.org/10.1029/JC092iC12p12947, 1987.

Olsen, A., Lange, N., Key, R. M., Tanhua, T., Bittig, H. C., Kozyr, A., Álvarez, M., Azetsu-Scott, K., Becker, S., Brown, P. J., Carter, B. R., Cotrim Da Cunha, L., Feely, R. A., Van Heuven, S., Hoppema, M., Ishii, M., Jeansson, E., Jutterström, S., Landa, C. S., Lauvset, S. K., Michaelis, P., Murata, A., Pérez, F. F., Pfeil, B., Schirnick, C., Steinfeldt, R., Suzuki, T., Tilbrook, B., Velo, A., Wanninkhof, R., and Woosley, R. J.: An updated version of the global interior ocean biogeochemical data product, GLODAPv2.2020, Earth Syst. Sci. Data, 12, 3653–3678, https://doi.org/10.5194/essd-12-3653-2020, 2020.

https://doi.org/10.5194/egusphere-2025-5945
Preprint. Discussion started: 15 December 2025

O'Mara, N. A., Cheung, A. H., Kelly, C. S., Sandwick, S., Herbert, T. D., Russell, J. M., Abella-Gutiérrez, J., Dee, S. G., Swarzenski, P. W., and Herguera, J. C.: Subtropical Pacific Ocean Temperature Fluctuations in the Common Era: Multidecadal Variability and Its Relationship With Southwestern North American Megadroughts, Geophys. Res. Lett., 46, 14662–14673, https://doi.org/10.1029/2019GL084828, 2019.

Phleger, F. B. and Soutar, A.: Production of Benthic Foraminifera in Three East Pacific Oxygen Minima, Micropaleontology, 19, 110, https://doi.org/10.2307/1484973, 1973.

Quay, P., Sonnerup, R., Westby, T., Stutsman, J., and McNichol, A.: Changes in the $^{13}C/^{12}C$ of dissolved inorganic carbon in the ocean as a tracer of anthropogenic CO_2 uptake: CHANGES IN THE $^{13}C/^{12}C$ OF DIC IN THE OCEAN, Glob. Biogeochem. Cycles, 17, 4-1-4–20, https://doi.org/10.1029/2001GB001817, 2003.

Quay, P., Sonnerup, R., Munro, D., and Sweeney, C.: Anthropogenic CO_2 accumulation and uptake rates in the Pacific Ocean based on changes in the $^{13}C/^{12}C$ of dissolved inorganic carbon, Glob. Biogeochem. Cycles, 31, 59–80, https://doi.org/10.1002/2016GB005460, 2017.

Racapé, V., Pierre, C., Metzl, N., Lo Monaco, C., Reverdin, G., Olsen, A., Morin, P., Vázquez-Rodríguez, M., Ríos, A. F., and Pérez, F. F.: Anthropogenic carbon changes in the Irminger Basin (1981–2006): Coupling δ13CDIC and DIC observations, J. Mar. Syst., 126, 24–32, https://doi.org/10.1016/j.jmarsys.2012.12.005, 2013.

Ravelo, A. C. and Fairbanks, R. G.: Oxygen Isotopic Composition of Multiple Species of Planktonic Foraminifera: Recorders of the Modern Photic Zone Temperature Gradient, Paleoceanography, 7, 815–831, https://doi.org/10.1029/92PA02092, 1992.

Rubino, M., Etheridge, D. M., Thornton, D. P., Howden, R., Allison, C. E., Francey, R. J., Langenfelds, R. L., Steele, L. P., Trudinger, C. M., Spencer, D. A., Curran, M. A. J., Van Ommen, T. D., and Smith, A. M.: Revised records of atmospheric trace gases CO₂, CH₄, N₂O, and <i>δ</i>¹³C-CO₂ over the last 2000 years from Law Dome, Antarctica, Earth Syst. Sci. Data, 11, 473–492, https://doi.org/10.5194/essd-11-473-2019, 2019.

Sabine, C. L., Feely, R. A., Gruber, N., Key, R. M., Lee, K., Bullister, J. L., Wanninkhof, R., Wong, C. S., Wallace, D. W. R., Tilbrook, B., Millero, F. J., Peng, T.-H., Kozyr, A., Ono, T., and Rios, A. F.: The Oceanic Sink for Anthropogenic CO_2, Science, 305, 367–371, https://doi.org/10.1126/science.1097403, 2004.

Sarmiento, J. L. and Gruber, N.: Sinks for Anthropogenic Carbon, Phys. Today, 55, 30–36, https://doi.org/10.1063/1.1510279, 2002.

Sautter, L. R. and Thunell, R. C.: Seasonal Variability in the $\delta^{18}O$ and $\delta^{13}C$ of Planktonic Foraminifera from an Upwelling Environment: Sediment Trap Results from the San Pedro Basin, Southern California Bight, Paleoceanography, 6, 307–334, https://doi.org/10.1029/91PA00385, 1991.

Spindler, M., Hemleben, C., Salomons, J. B., and Smit, L. P.: Feeding behavior of some planktonic foraminifers in laboratory cultures, J. Foraminifer. Res., 14, 237–249, https://doi.org/10.2113/gsjfr.14.4.237, 1984.

Sverdrup, H. U. and Allen, W. E.: Distribution of diatoms in relation to the character of water masses and currents off southern California in 1938, J. Mar. Res., 2, 131–144, 1939.

Tagliabue, A. and Bopp, L.: Towards understanding global variability in ocean carbon-13, Glob. Biogeochem. Cycles, 22, https://doi.org/10.1029/2007GB003037, 2008.

Takahashi, T., Sutherland, S. C., Sweeney, C., Poisson, A., Metzl, N., Tilbrook, B., Bates, N., Wanninkhof, R., Feely, R. A., Sabine, C., Olafsson, J., and Nojiri, Y.: Global sea–air CO2 flux based on climatological surface ocean pCO2, and seasonal biological and temperature effects, Deep Sea Res. Part II Top. Stud. Oceanogr., 49, 1601–1622, https://doi.org/10.1016/S0967-0645(02)00003-6, 2002.

https://doi.org/10.5194/egusphere-2025-5945
Preprint. Discussion started: 15 December 2025

459 Tans, P.: REMINISCING ON THE USE AND ABUSE OF ^{14}C AND ^{13}C IN ATMOSPHERIC CO_2, Radiocarbon,
460 64, 747–760, https://doi.org/10.1017/RDC.2022.7, 2022.

461 Thunell, R. C.: Seasonal and annual variability in particle fluxes in the Gulf of California: A response to climate
462 forcing, Deep Sea Res. Part Oceanogr. Res. Pap., 45, 2059–2083, https://doi.org/10.1016/S0967-0637(98)00053-3,
463 1998.

464 Global Monitoring Laboratory - Carbon Cycle Greenhouse Gases: https://gml.noaa.gov/ccgg/trends/data.html, last
465 access: 9 September 2024.

466 Van Geen, A., McCorkle, D. C., and Klinkhammer, G. P.: Sensitivity of the phosphate-cadmium-carbon isotope
467 relation in the ocean to cadmium removal by suboxic sediments, Paleoceanography, 10, 159–169,
468 https://doi.org/10.1029/94PA03352, 1995.

469 Wanninkhof, R., Park, G.-H., Takahashi, T., Sweeney, C., Feely, R., Nojiri, Y., Gruber, N., Doney, S. C., McKinley,
470 G. A., Lenton, A., Le Quéré, C., Heinze, C., Schwinger, J., Graven, H., and Khatiwala, S.: Global ocean carbon uptake:
471 magnitude, variability and trends, Biogeosciences, 10, 1983–2000, https://doi.org/10.5194/bg-10-1983-2013, 2013.

472 Wefer, G. and Berger, W. H.: Isotope paleontology: growth and composition of extant calcareous species, Mar. Geol.,
473 100, 207–248, https://doi.org/10.1016/0025-3227(91)90234-U, 1991.

474 Young, J. N., Bruggeman, J., Rickaby, R. E. M., Erez, J., and Conte, M.: Evidence for changes in carbon isotopic
475 fractionation by phytoplankton between 1960 and 2010: 50 YEAR RECORD OF GLOBAL SURFACE ε_p, Glob.
476 Biogeochem. Cycles, 27, 505–515, https://doi.org/10.1002/gbc.20045, 2013.